SAND2018-10344J

Deflagration-to-Detonation Transition In Bullseye Powder

Todd Miner, Devon Dalton, Dustin Romero, Matthew Heine, Allen Gorby

Steve Todd, and Blaine Asay

Sandia National Laboratories, 1515 Eubank Blvd SE, Albuquerque, NM 87123, USA

A series of compaction experiments was conducted to evaluate the mechanical, reactive, and deflagration-to-detonation transition behavior in Alliant Bullseye powder. Using a novel application of photon doppler velocimetry and light-fibers, the experiments measured both compaction and combustion waves in porous beds of Bullseye subjected to impact by gun-driven pistons. Relationships between initial piston velocity and transition distance are shown. Comparison is made between the Bullseye response and that found in classic Type I DDT.

I. INTRODUCTION

Many, but not all, explosive materials will undergo a transition to detonation when ignited by a flame or compression wave. This is referred to as a deflagration-to-detonation transition (DDT). Typical modes of transition include a strengthening of the initial disturbance through various processes until a shock is formed, and then a standard shock-to-detonation transition (SDT) occurs. The specific nature of the response differs, depending on the specific materials (e.g., propellants, ball powders, or explosives), and also the physical state (e.g., liquid, cast, pressed, or porous). For a given material, the distance required for the transition to occur is a function of many variables including the nature of initiation (e.g., flame, compression, friction etc.), type of confinement (e.g., steel, plastic), particle size and distribution, and initial density.

Scientific experimental studies of the DDT mechanism began in the early 1960's [1-3] and continued with work on propellants [4], ball powders[5], and various explosives [6-9]. The first comprehensive and experimentally-verified model of the process in a granular bed detailed how compression waves

coalesced and collapsed the material into a full-density compact, which resulted in the formation of a shock [10] . This was further corroborated by other work [11] which proposed two different modes of DDT; Types I and II. Type I occurs in beds with porosity up to ~30%, while Type II becomes important at porosities exceeding that value. A good review of both types can be found in reference [12].

The main parameters of interest to determine the mechanisms responsible for DDT are the trajectories of the compaction, combustion and detonation waves. Knowing these, the distance required for the process to progress from a deflagration to a detonation, x^*, can be determined. In addition, time-resolved densities and temperatures would be quite useful, but are very difficult to measure. Various techniques are used to observe the wave structures and histories. These include microwave interferometry, x-radiography, capped- and ionization shorting pins, light fibers, streak- and framing photography and high-speed videography. This study has utilized high-speed video along with light fibers and a novel application of photon doppler velocimetry (PDV).

Ignition of the explosive used in DDT studies can be achieved through various means. Glow plugs, thermite mixtures and hot wires have been used to directly thermally ignite the explosive. These methods have the advantage of being relatively simple to use. The disadvantage is that the ignition front can be nonuniform and the time of ignition ranges over a wide margin. Alternatively, pistons can be used to compress the material, causing ignition of the explosive through frictional forces at the piston face. This technique has the advantage of being more one-dimensional while suffering from the disadvantage of being slightly more complicated to field.

The capability of making accurate *a priori* predictions of DDT does not currently exist, although the problem has received serious attention for many years [13-16]. The main difficulty lies in the fact that the problem is both temporally and spatially multiscale, even in situations where quasi one-dimensional experiments are attempted. Additionally, combustion is a conductive process whereas detonation is not. Numerical calculations of these systems is exceedingly difficult, and no single hydrocode can currently do so. However, competent calculations have proven valuable in helping to

understand the mechanisms involved, as well as in attempts to design conditions that will prevent DDT from occurring in specific instances.

The limited ability to calculate the DDT process makes the collection of reliable data even more important. Accurate data are necessary in order to validate and verify numerical models, and to also enhance our understanding of the physical mechanisms responsible for the transition from a relatively mild reaction to one that is catastrophic. Additionally, data from a range of different materials are desirable so as to enable more widely applicable conclusions. The data presented here provide the most complete set of DDT data acquired to date, and thus should provide a reliable dataset against which to compare other experimental and modeling studies.

II. EXPERIMENTAL

A series of eight experiments was conducted using Alliant Bullseye powder (NC/NG/other, 58/40/2 w/w). The NC is nitrated to 13.25%. All experiments were conducted with a bed density of 0.68 g/cc. The powder was placed into a 4340 steel tube shown schematically in Fig 1. The material was introduced in small increments while tapping on the tube to allow normal settling to occur. The same amount of powder was used for all the experiments to ensure a consistent density throughout. For these studies a piston was used to ignite the explosive mixture. The piston was fit into the end of the tube (see Fig. **2**), and this was subsequently impacted by a projectile fired from a powder gun (see Fig. **3**). The gun used shot gun shells loaded into the breach with variable amounts of powder to achieve desired projectile velocities.

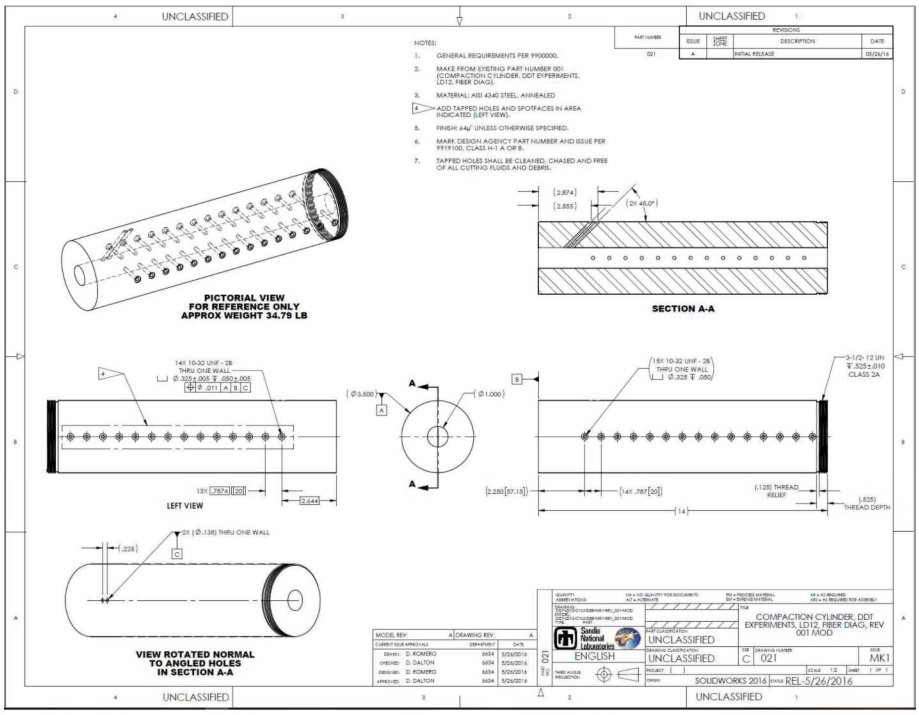

Fig 1. Schematic of tube

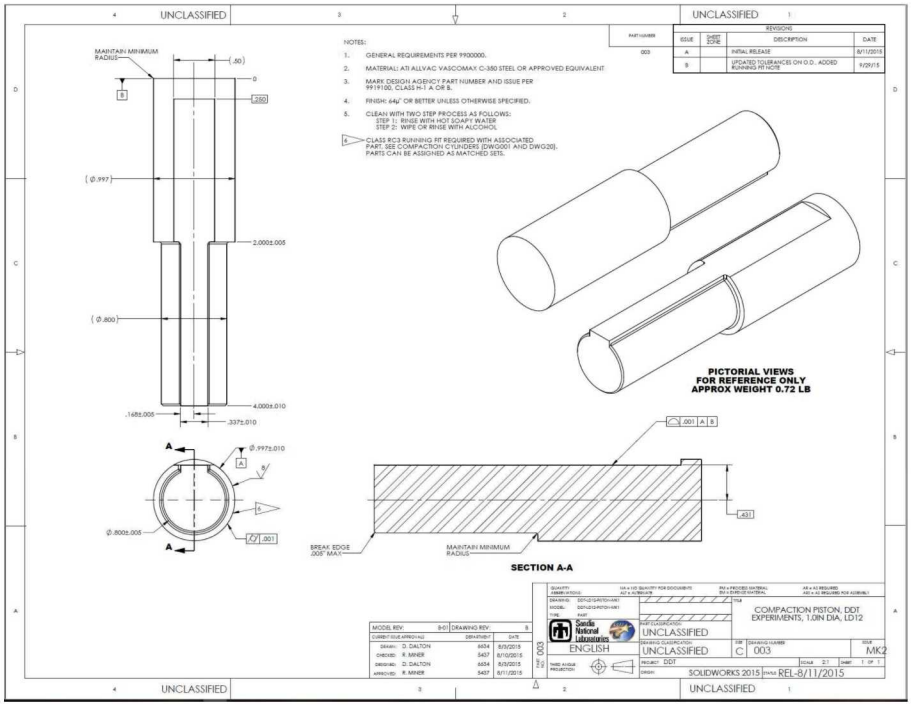

Fig. 2. Schematic of piston

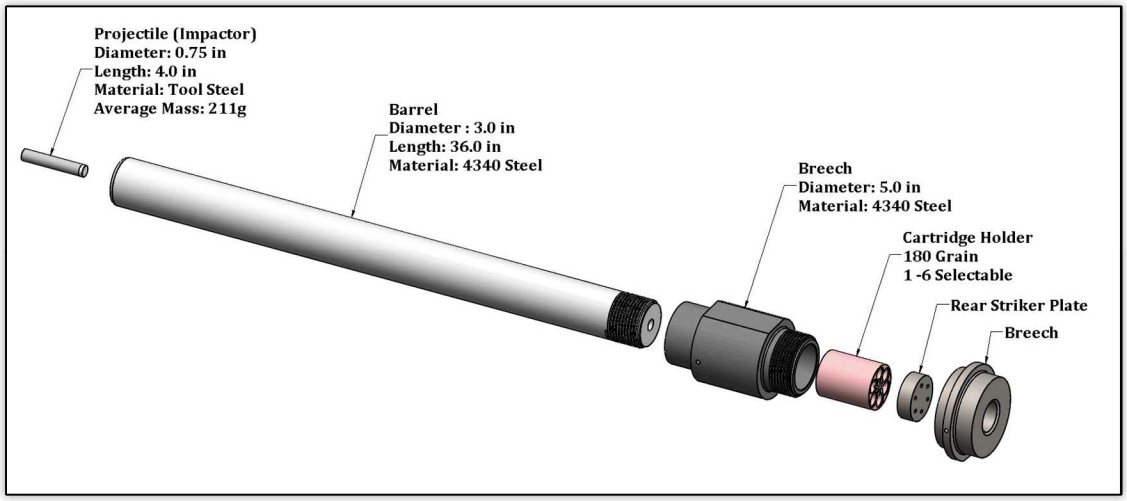

Fig. 3. Schematic of powder gun

The experiments were designed to separately track the (relatively) inert compaction waves, the combustion waves, and the detonation front. Light Fibers were used to follow the reactive waves, and PDV probes were used to track the compaction wave and detonation front. These were mounted on opposite sides of the cylinder at the locations shown in Fig. **4**. Distances shown are measured from the piston face.

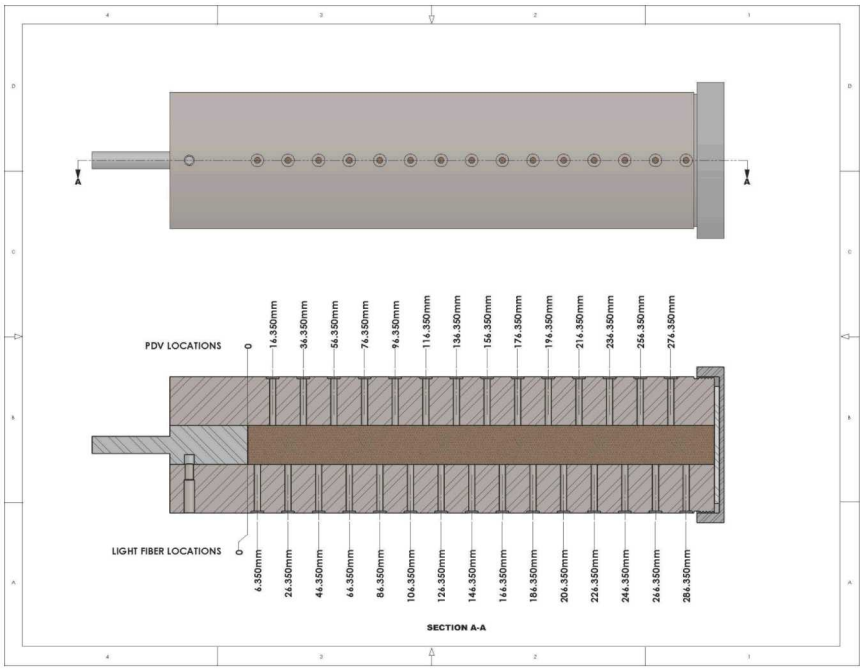

Fig. 4. Schematic of probe locations.

A Phantom Research V2511 video camera, sampling at rates from 170,000 fps to 310,000 fps, with exposures ranging from 0.71-1.00 us, and using either a 50mm or 85mm Nikon lens at f/5.6 was used to view each experiment. These images were used to gain an overall view of the tube expansion and progression of the reaction. Triggering was provided by a break wire stretched across the muzzle of the gun. Illumination was provided using 2 flash bulbs.

In a unique application of PDV, probes were placed perpendicular to the motion of the compaction wave. Rather than viewing a plate moving towards the probe as in the typical use of this diagnostic, the PDV probes in these experiments observed motion of the grains transverse to the probe. In this case, PDV acted as a time of arrival gauge that monitored the position of the compaction wave.

The time-of-arrival (TOA) PDV probes are significantly simpler than the collimating probe design. The back-reflection created from the cleaved surface of the single mode SMF28 fiber used in the system

is strong enough to serve as a diagnostic interface on the material surface. The probes are assembled by cutting a 5-meter fiber jumper in half, stripping the protective jacket and Kevlar strength member, and gluing the cut end into a drilled nylon #10-32 socket head cap screw. After bonding into the screw, the fiber end is cleaved flush with the screw face, as flat as possible to maximize the back-reflection. Any disruption to this interface during the experiment, such as a compaction wave, results in a notable change in light return to the PDV system. A detonation wave at the interface creates a complete loss of light acting as a distinct timing fiducial.

In addition to monitoring the compaction wave arrival, PDV was also used to measure the piston velocity. This was monitored via a collimating probe placed at a 45° angle relative to a flat machined on the piston itself (see Fig. **5**). Reflective tape was placed on the piston flat to provide a stronger return signal. The signal was recorded until the reflective portion of the piston was compromised which happened at various times, depending on a number of external factors. Thus, the end of the PDV record was not an indication of the end of piston motion.

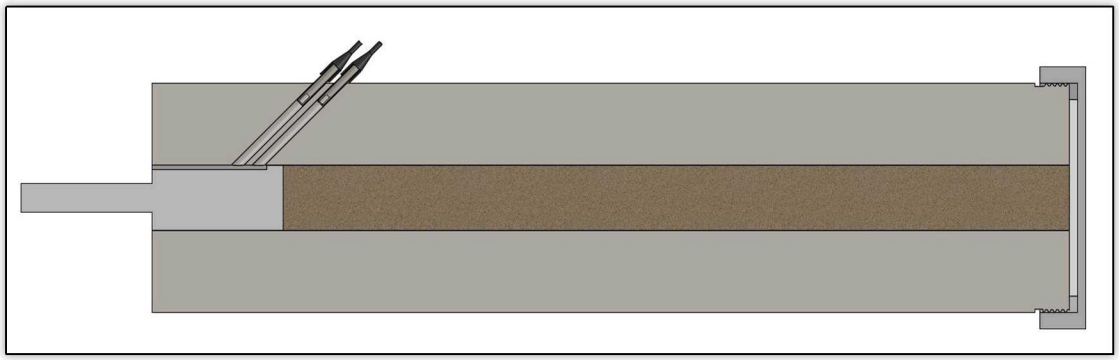

Fig. 5. Locations of PDV probe to measure piston velocity

A second diagnostic used to track the light-emitting combustion and detonation waves was the optical time of arrival system. A group of broadband optical detectors coupled with large plastic core (1 mm) multimode fibers was found to be quite effective. Thorlabs PDA10A Silicon amplified detectors

with 150 MHz bandwidth and a wavelength range from 200-1100nm were used. Light generated during detonation created large signals (2-10 volts) with relatively short rise times (~50ns).

III. RESULTS

Error! Reference source not found. summarizes the data, including the resultant linearized piston and compaction velocities. These velocities were not constant, but for a majority of travel distance were only mildly decelerating. The values reported here are linear fits of the quasi-steady portions for comparison to other experiments. The full records of velocity as a function of time will be presented next.

TABLE I. Summary of experimental results with t_0 being the signal arising from the break-wire located at the end of the gas gun barrel

Shot Number	Projectile Velocity (m/s)	Piston Velocity (m/s)	Compaction Velocity (m/s)	Detonation Velocity (mm/μs)	Transition Distance (x^* mm)
1	421	182	N/A	4.0	70
2	340	164	290	4.2	81
3	334	150	301	4.1	93
4	150	94	182	4.5	156
5	100	57	150[a], 130[b]	4.5	206
6	~54	19	100[c]	N/A	N/A
7	M16 det.	N/A	N/A	4.2	26-36[d]
8	130	68	135	4.3	176

a) at 1500 μs.

b) at 2500 μs.

c) at 2500 μs.

d) this is the estimated run-up distance arising from 0.241-in diameter detonator

Fig. **6** shows a graphical compilation of all the data from the eight experiments. The PDV probes recorded both the initial compaction wave and also the stronger shock wave that occurred later, after initiation of vigorous reaction and detonation. These late-time signals correspond very closely with those from the light fibers.

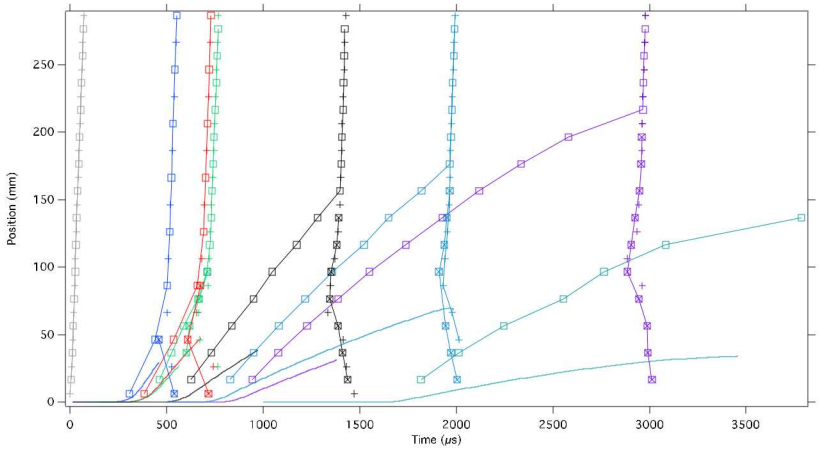

Fig. 6. Compilation of all experimental data. The square symbols are PDV signals, the plus symbols are for light fibers, and the lines with no symbols represent the piston trajectory. Lines are drawn

between PDV and light fiber data points to guide the eye. Piston trajectory is a continuous measurement. Note that the end of the piston position record denotes the loss of PDV signal, not cessation of piston motion.

Fig. **7** shows the same data as found in Fig 6 except that the late-time PDV data have been removed for clarity to emphasize the light fiber signals.

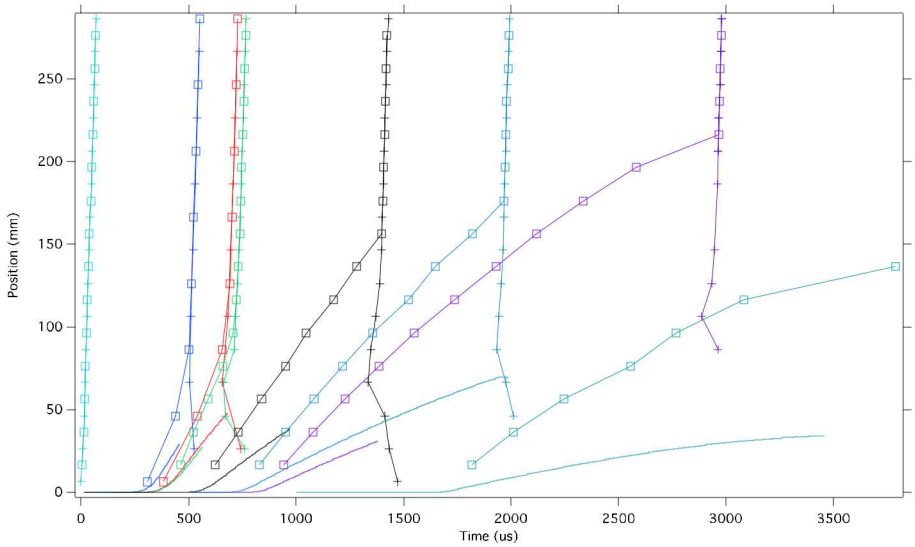

Fig. 7. Compilation of experimental data with late-time PDV data removed for clarity. The square symbols are PDV signals, the plus symbols are for light fibers, and the lines with no symbols represent the piston trajectory. Lines are drawn between PDV and light fiber data points to guide the eye. Piston trajectory is a continuous measurement. Note that the end of the piston position record denotes the loss of PDV signal, not cessation of piston motion.

All of the experiments had a common trigger; a break-wire at the end of the gun barrel. Thus, the arrival time of the projectile at the piston surface is a function of the projectile velocity. To make a 1:1 comparison among the data,

Fig. 8 shows the PDV data shifted so that the beginning of piston motion of all the experiments corresponds to start of piston motion of shot 1. This choice of starting time is completely arbitrary, but provides a common time that makes comparison of behavior between different experiments more straightforward.

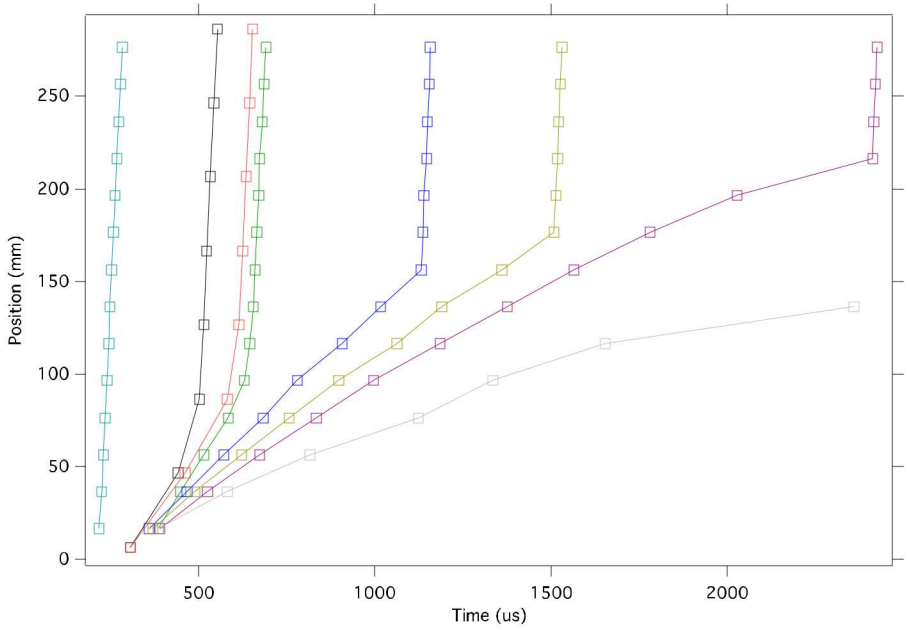

Fig. 8. PDV data shifted to match initial piston motion of shot 1.

Transition distance (x^*) is defined as the distance required to achieve a detonation with a given piston velocity. It can be measured in different ways depending on the experimental configuration. For these tests, a line was extrapolated along the compaction wave PDV data and intersected with a line drawn along the PDV data corresponding to the detonation wave. The true location of transition is before this point, but for comparison purposes this method provides reliable data. Fig. **9** shows the transition distance (x^*) vs linearized piston velocity.

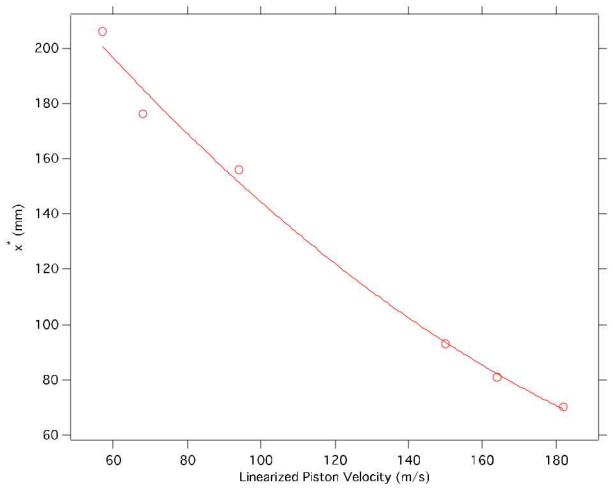

Fig. 9. Linearized piston velocity vs x^* with data fit using quadratic function: $x^* = 293.46 - 1.8092\,x + 0.0031728x^2$

Shot 7 used an identically packed and instrumented tube as in previous tests but an M16 detonator was placed at the piston face and no gas gun projectile was fired. This test provides a baseline which demonstrates the behavior of the gun powder upon prompt initiation. As can be seen in Fig. **10**, detonation was not instantaneous, but a run-up distance was obtained. This provides a data point similar to that obtained in a pop plot, but in this case, the input wave geometry is three dimensional instead of one dimensional. However, these data provide an estimate of the run-up distance in this configuration.

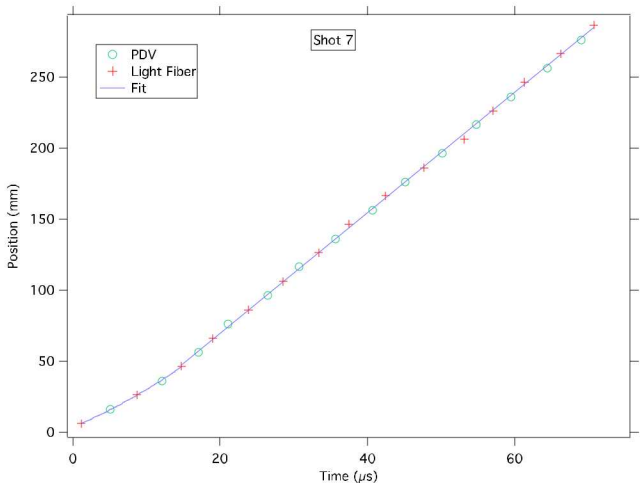

Fig. 10. Data from Shot 7. Quadratic fit to first 3 light fiber points, linear fit to remainder.

Finally, the time difference between the compaction wave PDV data and the light fiber data was measured. These data are equivalent to an induction time since the combustion begins once the piston begins compressing the powder. However, light does not appear until the combustion achieves a certain critical rate. Because the light fibers and PDV probes are at different axial locations, we averaged the PDV times to estimate the wave arrival at the light fiber locations, assuming a linear velocity. The difference between the two times was then plotted against the light fiber positions as shown in Fig. **11**. As can be seen, the induction time lengthens as the piston velocity decreases, as expected.

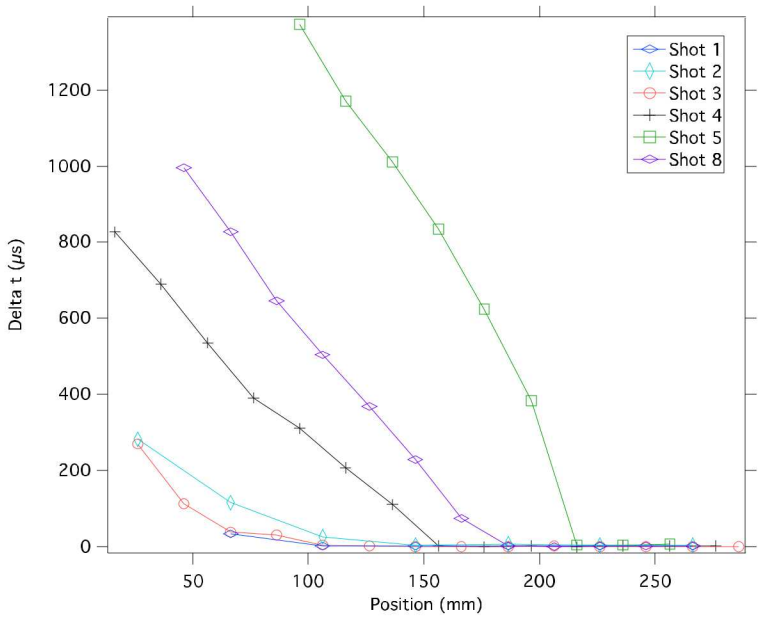

Fig. 11. Induction times for each experiment.

IV. DISCUSSION

DDT can occur in gases, particle-laden flows, porous beds at various compactions, or in full-density beds. DDT in each of these environments proceeds by a pathway that has some similarities and also some differences from each of the others. In packed beds of similar densities to those found in this study, Type 1 DDT is the mechanism by which the transition has been found to occur. Fig. **12** depicts the generalized Type 1 mechanism [12].

The compaction wave (c) is driven by the piston. After some amount of time combustion begins at the piston face. As the combustion intensifies, the pressure rises and acoustic waves move forward. These can be thought of as characteristics, each one having a higher velocity than the last. At some point these waves coalesce and overcome the strength of the bed, which then collapses to create a region of full-density. The velocity at the top of this fully-compressed region begins to accelerate and eventually forms a shock, which then transitions to a detonation. This detonation runs at the velocity characteristic of the compacted material. When it intersects the compaction wave, the detonation velocity falls to that expected in the porous bed.

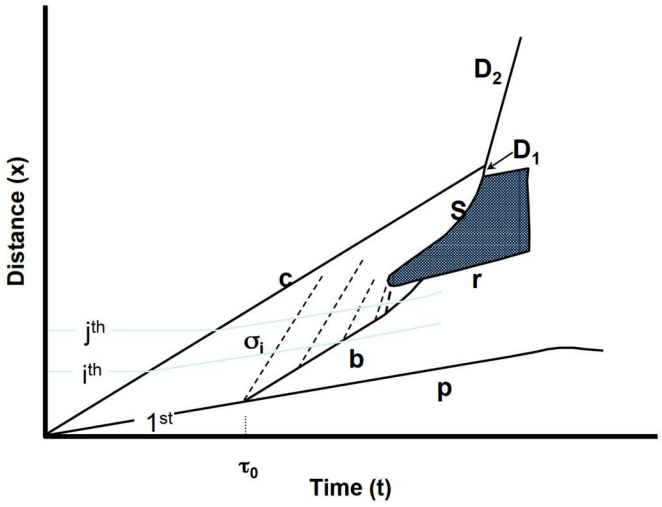

Fig. 12. Schematic of Type 1 DDT [12].

The timing and location of each of these events is entirely dependent on the specific energetic material, the density, confinement, available volume and temperature. However, if one examines the data from the current experiments, the similarities to the standard depiction is evident (see Fig. **13**).

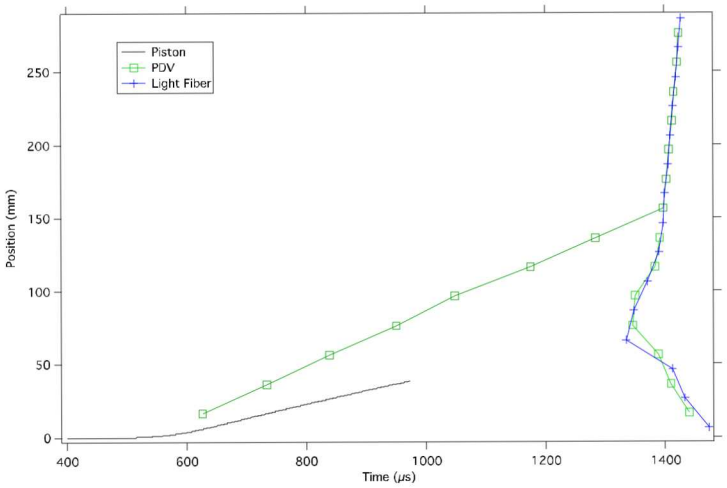

a)

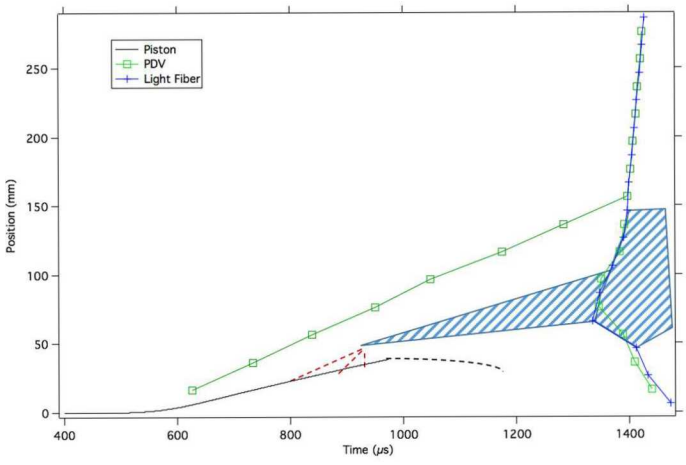

b)

Fig. 13. (a) Shot 4 x(t) and (b) x(t) with notional waves drawn in.

Without more finely resolved diagnostics, we cannot say what the structure actually is. However, nothing that we have observed contradicts the conclusion that this is a Type 1 DDT process.

The results from these experiments were used to calibrate existing distended material shock compaction models and to link them to a newly-developed reactive burn model. We are evaluating this approach to simulate the type of mechanical insults to porous non-ideal explosives described here. The initial results from the numerical simulations are very promising and are being prepared for publication.

V. CONCLUSIONS

We have completed a series of DDT experiments with carefully controlled boundary conditions. The data demonstrate the response of a porous bed of Bullseye with behavior ranging from prompt detonation to an inert compaction wave. We have shown that the behavior is similar to that observed in Type 1 DDT. While the temporal and spatial resolution of the data are not sufficient to conclusively prove that all the structures observed in Type 1 DDT are indeed present, we have high confidence in the resolution of the compaction and burn fronts and that these data can be used for model development and validation. Moreover, we demonstrated the repeatability of generating a DDT with Bullseye propellant and its usefulness for future DDT empirical analysis.

ACKNOWLEDGEMENTS

Sandia National Laboratories is a multi-mission laboratory managed and operated by National Technology & Engineering Solutions of Sandia, LLC, a wholly owned subsidiary of Honeywell International Inc., for the U.S. Department of Energy's National Nuclear Security Administration under contract DE-NA0003525. This paper describes objective technical results and analysis. Any subjective views or opinions that might be expressed in the paper do not necessarily represent the views of the U.S. Department of Energy or the United States Government.

REFERENCES

1. Gipson, R.W. and A. Maček, *Flame fronts and compression waves during transition from deflagration to detonation in solids.* Symposium (International) on Combustion, 1961. **8**(1): p. 847-854.

2. Griffiths, N. and J.M. Groocock, *814. The burning to detonation of solid explosives.* Journal of the Chemical Society (Resumed), 1960(0): p. 4154-4162.

3. Maček, A., *Transition from Deflagration to Detonation in Cast Explosives.* The Journal of Chemical Physics, 1959. **31**(1): p. 162-167.

4. Bernecker, R.R., W.W. Sandusky, and A.R. Clairmont. *Deflagration-to-Detonation Transition of a Double Base Propellant*. in *Eighth Symposium (International) on Detonation*. 1985. Albuquerque, NM.

5. Samirant, M. *DDT in RDX and Ball Powder*. in *Eighth Symposium (International) on Detonation*. 1985. Albuquerque, NM.

6. Gifford, M.J., *A mechanism for the deflagration-to-detonation transition in ultrafine granular explosives*, in *AIP Conference Proceedings*. 2000. p. 845-848.

7. McAfee, J.M., B.W. Asay, and J.B. Bdzil. *Deflagration-to-detonation in granular HMX: Ignition, kinetics, and shock formation*. in *Tenth Symposium (International) on Detonation*. 1993. Boston, MA.

8. Smilowitz, L., et al., *The evolution of solid density within a thermal explosion II. Dynamic proton radiography of cracking and solid consumption by burning.* Journal of Applied Physics, 2012. **111**(10).

9. Tringe, J.W., et al., *Observation and modeling of deflagration-to-detonation transition (DDT) in low-density HMX*, in *Shock Compression Of Condensed Matter - 2015: Proceedings of the Conference of the American Physical Society Topical Group on Shock Compression of Condensed Matter*. 2017: Tampa, FL.

10. McAfee, J.M., et al. *The deflagration-to-detonation transition in granular HMX*. in *9th Symposium (International) on Detonation*. 1991. Portland, OR.

11. Luebcke, P.E., P.M. Dickson, and J.E. Field, *Deflagration-to-detonation transition in granular pentaerythritol tetranitrate.* Journal of Applied Physics, 1996. **79**(7): p. 3499-3503.

12. Asay, B., *Shock Wave Science and Technology Reference Library, Vol. 5: Non-Shock Initiation of Explosives*. Vol. 5. 2010, Berlin: Springer.

13. Asay, B.W., S.F. Son, and J.B. Bdzil, *The role of gas permeation in convective burning.* International Journal of Multiphase Flow, 1996. **22**(5): p. 923-952.

14. Dong, H., et al., *Numerical simulation of deflagration to detonation transition in granular HMX explosives under thermal ignition.* Journal of Thermal Analysis and Calorimetry, 2016. **127**(1): p. 975-981.

15. Ermolaev, B.S., et al., *Nonideal regimes of deflagration and detonation of black powder.* Russian Journal of Physical Chemistry B, 2010. **4**(3): p. 428-439.

16. Son, S.F., B.W. Asay, and J.B. Bdzil, *Inert plug formation in the DDT of granular energetic materials*, in *AIP Conference Proceedings*. 1996. p. 441-444.